BMB Reports - Manuscript Submission

Manuscript Draft

Manuscript Number: BMB-17-084

Title: Heterogeneous interaction network of yeast prions and remodeling factors detected in live cells

Article Type: Article

Keywords: yeast prions; remodeling factors; fluorescence cross-correlation spectroscopy; live cell; protein interaction

Corresponding Author: Chan-Gi Pack

Authors: Chan-Gi Pack[1,*], Yuji Inoue[2,3], Takashi Higurashi[3], Shigeko Kawai-Noma[2], Daigo Hayashi[2], Elizabeth Craig[3], Hideki Taguchi[2]

Institution: [1]Asan Institute for Life Sciences, Asan Medical Center, University of Ulsan College of Medicine,
[2]Department of Biomolecular Engineering, Tokyo Institute of Technology,
[3]Department of Biochemistry, University of Wisconsin,
[4]Department of Virology, Osaka University,

Manuscript Type: Article

Title: Heterogeneous interaction network of yeast prions and remodeling factors detected in live cells

Author's Name: Chan-Gi Pack[1,*], Yuji Inoue[2,#], Takashi Higurashi[3], Shigeko Kawai-Noma[2], Daigo Hayashi[2], Elizabeth Craig[3], Hideki Taguchi[2]

Affiliation: [1] Asan Institute for Life Sciences, Asan Medical Center & Department of Convergence Medicine, University of Ulsan College of Medicine, Seoul 05505, Republic of Korea. [2] Department of Biomolecular Engineering, Graduate School of Biosciences and Biotechnology, Tokyo Institute of Technology, B56, 4259 Nagatsuta, Midori-ku, Yokohama 226-8501, Japan. [3] Department of Biochemistry, University of Wisconsin, 433 Babcock Drive Madison, WI 53706, USA. [#] Present address: Department of Virology, Research Center for Infectious Diseases Control, Research Institute of Microbial Diseases, Osaka University, 3-1 Yamadaoka, Suita, Osaka, 565-0871, Japan

* Corresponding author

Running Title: Interaction network of yeast prions in live cells

Keywords: yeast prions, remodeling factors, fluorescence cross-correlation spectroscopy, live cell, protein interaction

Corresponding Author's Information: Chan-Gi Pack (Tel: 82-2-3010-8611, Fax:82-2-3010-4182, E-Mail: changipack@amc.seoul.kr)

ABSTRACT

Budding yeast has at least dozens of prions, which are mutually dependent on each other for the *de novo* prion formation. In addition to the interactions among prions, transmissions of prions are strictly dependent on two chaperone systems: Hsp104 and the Hsp70/Hsp40 (J-protein) system, both of which cooperatively remodel the prion aggregates to ensure the multiplication of prion entities. Since it has been postulated that prions and the remodeling factors constitute complex networks in cells, a quantitative approach to describe the interactions in live cells would be required. Here, we applied the dual-color fluorescence cross-correlation spectroscopy to investigate the molecular network of interaction in single live cells. The findings demonstrate that yeast prions and remodeling factors constitute a network each other through heterogeneous protein-protein interactions.

INTRODUCTION

Prions are protein-based infectious factors (1). In the prion, the altered conformation of a protein converts the normal structure to the altered form, resulting in the formation of ordered aggregates called amyloids (1). Although this prion concept was originally developed for mammalian neurodegenerative diseases, such as scrapie, this concept has been applied to non-Mendelian genetic elements in budding yeast cells, [*PSI*$^+$] and [*URE3*] (2). In [*PSI*$^+$] and [*URE3*] cells, amyloid structures of Sup35 and Ure2 are the prion determinants and are transmitted to daughter cells through a dynamic remodeling of the amyloid aggregates (3-8). Extensive studies using genetically tractable budding yeast as a model system have revealed that more than several dozen yeast proteins, including Rnq1, New1 and Swi1, behave as prions (9-14).

Although amyloids are kinds of homo-oligomers formed *via* cross-beta interactions, yeast prions are related each other in *de novo* formation and transmission. Regarding *de novo* formation, it has been demonstrated that prions affect the appearance of other prions (10, 15). As a well-known example, the prion form of Rnq1 is required for the *de novo* appearance of [*PSI*$^+$], and *vice versa* (10, 15). Therefore, it has been suggested that there are interactions among prions either in a direct or indirect manner. In addition to the mutual dependence among prions, the transmission of yeast prions is strictly dependent on two chaperone systems: Hsp104 and the Hsp70/Hsp40 (J-protein) system. Hsp104, which is a homohexameric ATPase involved in the thermotolerance of yeast, is an essential factor to maintain yeast prions (16, 17). Unlike Hsp104, which is unique in yeast, the Hsp70/Hsp40 system is diverse (18). An essential J-protein Sis1 (Hsp40), cochaperone of Ssa Hsp70, is a critical factor for the transmission of several yeast prions, including [*PSI*$^+$] (19, 20). Hsp104, a molecular disaggregase, remodels the amyloid aggregates to ensure the multiplication of prion entities in cooperation with the Hsp70/Hsp40 system (18, 21-23).

As described above, it seems that prions are in a complex network with the assistance of remodeling factors to propagate and transmit in the cells. To better understand the protein network, it would be important to quantitatively detect the physical interaction among the prions and/or between prions and the remodeling factors. In fact, previous studies have reported physical interactions among prions as well as between prions and the remodeling factors in lysates and in cells (24, 25). Affinity purification of Sup35 aggregates from [*PSI*$^+$] lysates to identify associated proteins revealed that the Sup35 aggregates contained Rnq1, and that the major components of [*PSI*$^+$] aggregates were Sup35 and Ssa1/2 (Hsp70) (25, 26).

Fluorescence microscopic imaging of GFP- or RFP-tagged prions and remodeling factors was also used for detecting colocalzation of the proteins on a large and immobile aggregate formed in live prion cells (27-30). However, there is no quantitative analysis of such interactions between mobile proteins in other regions of live cells surrounding the immobile aggregate.

In this study, we applied fluorescence correlation spectroscopy (FCS) and fluorescence cross correlation spectroscopy (FCCS) to detect the interaction network of related proteins in single live cells. FCS is a technique used to determine the diffusional mobility of fluorescence molecules, providing us information about the size of the molecules, which is suitable to investigate the prions by discriminating prion aggregates from the monomeric state (31-34). Additionally, FCCS is an advanced FCS method that uses two different colored proteins to directly detect an interaction between the proteins in addition to the acquisition of each of the FCS parameters of the two proteins (35). Since FCS and FCCS are usually combined with confocal laser scanning microscopy (CLSM), we can define the detection volume at any position of interest inside cells in a noninvasive manner. Interestingly, FCS and FCCS successfully detected the physical interaction among prions (Sup35, Ure2, Rnq1, New1) and remodeling factors (Hsp104 and Sis1) in the freely mobile and oligomer states, and showed that they specifically interacted with each other in yeast cells in the prion state. These results suggest that there is a dynamic and heterogeneous network of prions and remodeling factors composed of various physical interactions.

RESULTS

FCS analysis of the hydrodynamic properties of yeast prions and the remodeling factors

Previous studies based on CLSM observation combined with FCS have already demonstrated that FCS is a powerful method to discriminate prion oligomers (i.e. small and mobile aggregates) from the monomeric form by quantitative analysis of diffusional behavior of the GFP-tagged N and M prion domains of Sup35 (Sup35NM-GFP) and the intact Sup35 containing GFP (Sup35NGMC) (31-33). In this study, we further characterized diffusional behaviors of the Sup35 variants and other yeast prions such as Rnq1, Ure2 and New1, and representative remodeling factors, Hsp104 and Sis1 (Table S1).

The diffusion coefficients (*D*s) of each protein in supernatant solution obtained from cell lysates and the cytosol of live cells were summarized in Table 1. Monomer GFP (mGFP) in lysis solution prepared from non-prion [*psi*$^-$] and prion [*PSI*$^+$] cells show a single *D* value expected from their molecular weights in spherical shape, indicating that mGFP molecules diffuse in a monomeric state without aggregates (Fig.1A *black*, Table S1). Only one diffusional component was detected in the lysis solution of the yeast prion proteins from non-prion [*psi*$^-$] ([*gpsi*$^-$]) cell lysate (Fig.1A *blue and red*, Table S1), even though the diffusion of Sup35NM-GFP (Sup35NGMC) was slower than expected as calculated from its theoretical molecular weight. In addition to our previous study (31), this result suggests that monomers diffuse in a nonspherical shape.

In contrast, two diffusional components were detected in the lysis solution of the yeast prion proteins from prion cells (Table 1). Fast diffusions of the proteins from yeast prion cells, represented by D_{fast}, corresponded to the diffusions of the proteins in lysis solution from non-prion cells and constituted a small proportion, ranging from 9 to 30%. Slow diffusions of the proteins, represented by D_{slow}, corresponded with large spherical complexes with hydrodynamic sizes ranging from 60 to 500MD and covered a large proportion of lysis samples, ranging from 70 to 91%. It is notable that the molecular weight of the large complexes can be much smaller than the estimated values if the molecular shape of the complexes is not spherical, but rod-like (32).

For cellular analysis, FCS measurements for yeast prion proteins were carried out on the other positions of cells surrounding a dot-like immobile aggregate (fluorescent foci) (31, 33). Fast diffusion occupied a large proportion of the cellular diffusion of mGFP in [*psi*$^-$] cells and was well characterized by their

hydrodynamic size as demonstrated in previous study (Fig. 1B *gray*) (31). Diffusions of Sup35NM-GFP in [*psi*$^-$] and Sup35NGMC in [*gpsi*$^-$] cells also consisted of a large proportion of fast diffusion ranging from 85 to 90%. Although the D_{fast} values of the two proteins were slightly smaller than those expected from the *D* values in lysis solution and cellular viscosity (Fig.1B *black* and *green*, Table 1), it is suggested that the fast diffusions present monomeric states of each protein, respectively. Slow diffusions of mGFP and yeast prion proteins equally occupied a small proportion ranging from 10 to 15%, and D_{slow} values were not different from each other. Slow diffusion detected in non-prion cells could have originated from a non-specific cellular interaction or from very slow photobleaching of GFP (35).

The diffusions of Sup35NM-GFP and Sup35NGMC in [*PSI*$^+$] and [*GPSI*$^+$] cells were much slower than those of the Sup35 molecules in the non-prion cells, indicating that large oligomers were detected and the diffusions were mainly represented by a large proportion of the mobile oligomers (Fig. 1B *blue* and *red*). The diffusion profiles (i.e. FAFs) of Sup35NM-GFP were different from those of Sup35NGMC. Distribution of D_{fast} and D_{slow} values obtained from [*PSI*$^+$] cells were not much different from those of [*GPSI*$^+$] cells (Fig. 1C, D). Instead, the distribution of the fractional ratio of D_{fast} and D_{slow} was largely different between [*PSI*$^+$] and [*GPSI*$^+$] cells. The large difference could be explained by the abundance of Sup35 proteins, since Sup35NM-GFP was overexpressed whereas Sup35NGMC was endogenously expressed. In practice, it was found that the concentration of overexpressed Sup35NM-GFP was 2.4-fold higher than that of endogenous Sup35NGMC for non-prion cells (Table S2). Therefore, the number of Sup35NM-GFP aggregates in a cell would be relatively higher than that of the Sup35NGMC aggregates. Alternatively, the difference of expression could reflect the tendency to form foci: Sup35NMGFP might be more prone to form amyloids than Sup35NGMC, resulting in accumulation of Sup35NM-GFP oligomers and formation of foci with the fibrillar structure (31-33). The result demonstrates that the hydrodynamic property (i.e. size) of Sup35 aggregates (the mobile oligomers) in the prion cells are almost the same regardless of the expression level of Sup35-GFP. Rnq1 tagged with mGFP (Rnq1-GFP) was also characterized using FCS (Fig. S1, Table 1), and the diffusion profile were comparable to those of Sup35NM-GFP or Sup35NGMC (Table 1). Our results suggest that the biochemical balance between elongation and fragmentation of amyloids might be common among yeast prions.

We also expressed Hsp104-mCherry (Hsp104-GFP) or Sis1-mCherry, which are known as prion-remodeling factors in non-prion cells. FCS analyses showed that around half of Hsp104-GFP and Sis1-mCherry molecules diffused very slowly, even in non-prion cells (Fig. S2, Table 1). The D_{slow} values for Hsp104-GFP and Sis1-mCherry were 0.34 and 0.6 $\mu m^2/s$, respectively. The values were 30-fold slower than the diffusion coefficient of those proteins in the lysates (Table 1). The slow diffusions of Hsp104 and Sis1 in non-prion cells may result from a strong interaction with an immobile cellular compartment, such as the cytoskeleton.

Consequently, FCS analysis demonstrated that a large proportion of mobile and small aggregates or oligomers in yeast prion cells exists in the other region of cells surrounding an immobile large aggregate. Moreover, the hydrodynamic property of oligomers in live cells can be fully differentiated from monomer molecules.

FCCS analysis of the interactions among prions in live cells

Yeast genetic experiments have suggested that there are interactions among prions as well as between prions and remodeling factors such as Hsp104. In fact, fluorescence microscopic studies based on confocal imaging using GFP and RFP confirmed colocalizations of prion protein and remodeling factor, such as Sup35-Rnq1 or Sup35-Hsp104. It was suggested that transmission or propagation of the prion state is accomplished by the dynamic property of prion oligomers, such as diffusion and rapid transmission of small oligomers from mother cell to daughter cell (31). Nevertheless, the interactions were only observed in highly bright and very large foci, and the details of the physical interactions between them in living cells are still unclear. It is clear that interactions between highly mobile monomeric and oligomeric proteins in live cells are hardly traceable by conventional imaging methods such as confocal microscopy. Therefore, we applied the CLSM-based FCCS technique to investigate the physical interactions among highly mobile prions and remodeling factors.

Firstly, we examined interactions among prions, using Sup35NGMC with overexpressed RFP (mCherry or TagRFP), TagRFP tagged Sup35NM, Ure2N, Rnq1C, and New1N prion domains in [*gpsi*$^-$] or [*GPSI*$^+$] cells (Fig. 2 and Fig. S3). Fig. 2A and 2B show representative confocal images of cells co-expressing TagRFP- and GFP-tagged proteins, time traces of average fluorescence intensities, and corresponding

correlation functions. The correlation function, G(τ), contain two auto-correlation functions (*blue* and *red*), which represent the behaviors of individual proteins, and one cross-correlation function (*black*), which represents the co-diffusion of two fluorescent proteins (i.e. physical interaction, *see also Methods section*). FCCS analysis between Sup35NGMC and TagRFP-tagged Sup35NM in [*gpsi*$^-$] cells showed only background levels of relative cross-correlation amplitude (Fig. 2A). In contrast, a high positive RCA value was detected in the analysis of Sup35NGMC and Sup35NM -TagRFP in [*GPSI*$^+$] cells (Fig. 2B), indicating that Sup35 molecules strongly interact with each other and form stable oligomers in the prion cells. In addition, cross-correlation signals between Sup35-GFP and other prion proteins tagged with TagRFP in [*gpsi*$^-$] cells showed RCA values similar with background levels, whereas those in [*GPSI*$^+$] cells showed all high RCA values (Fig. S3A ~ D). This result indicates that Sup35 and other prion proteins also strongly interact with each other (Fig. 2C).

FCCS analysis of the interactions between prions and remodeling factors in live cells

Secondly, the interactions of Sup35 with two remodeling factors, Hsp104 and Sis1, were examined (Fig. 3). FCCS analysis revealed a strong interaction between Sup35NM-GFP and Sis1-mCherry as well as Hsp104-mCherry in prion cells (*black* curves in Fig. 3A, B). In [*psi*$^-$] ([*gpsi*$^-$]) non-prion cells, much small values of mean RCA were observed (Fig. 3C, D and Fig. S3E, F). Moreover, FCCS showed a strong interaction between Rnq1-GFP and Sis1-mCherry in [*RNQ*$^+$] cells, while no significant RCA value was detected in [*rnq*$^-$] cells (Fig. 3C). This result demonstrates that the interaction of Sup35 with remodeling factors depends on the prion state in cells. Histograms of RCA in Sis1-Sup35 or Sis1-Rnq1 analyses showed that the overall RCA values in Sis1-Rnq1 were higher than those in Sis1-Sup35 (Fig. S4), even though the mean values of RCA were similar to each other. This suggests that the remodeling factor, Sis1, binds to Rnq1 in a more stable manner than Sup35. FCCS also revealed a significant interaction between Sup35 and Hsp104 (Fig. 3D). The mean values of RCA for the interaction between Sis1 and Sup35 (or Rnq1) were larger than those between Hsp104 and Sup35 (or Rnq1) (Fig. 3C, 3D). This finding is consistent with previous studies, in which Sis1 are preferentially bound to Sup35 or Rnq1 aggregates (20, 25). Since GdnHCl is known to cure [*PSI*$^+$] due to the perturbation of Hsp104 as shown by FCS analyses of single cells (33), we measured FCCS for the interaction between Sup35-Hsp104 in GdnHCl-treated [*GPSI*$^+$] cells.

Strikingly, the mean values of RCA were gradually reduced with incubation time after GdnHCl treatment (Fig. 3D) and the fractional ratio of D_{slow} was also reduced from 53% into 15% after 48 hr. The result indicates that the reduction of RCA values is correlated with the decrement of fractional ratio of D_{slow} component (33). The result supports that GdnHCl treatment could inactivate Hsp104 through inhibition of the interaction between Hsp104 and Sup35 oligomers, eventually leading to the curing of [*PSI*$^{+}$] (22, 33).

DISCUSSION

Previous genetic experiments showed that there are interactions between prions (10). However, study based on genetics could not directly answer whether those interactions are due to the physical prion-prion interactions or an indirect consequence via trans-acting factors like remodeling factors. Although colocalization analysis of fluorescent foci of prion proteins in cells has already suggested a direct association of a prion with other types of prion (27, 28), such confocal imaging-based analysis cannot examine highly mobile and small prion oligomers. It is emphasized that FCCS analysis clearly demonstrated that strong physical interactions among prions existed in cells under the condition where those prions were freely diffuse as oligomers in the cytoplasm.

We note that prion-prion interactions were only detected in prion cells, but not in non-prion cells. The result demonstrates that prion interactions are dependent on the amyloid states, and then suggests that prion-induced *de novo* formation of other prion is due to a cross-seeding mechanism (8), by which pre-existing amyloids were used as seeds of other prion proteins. Moreover, comparison of the RCA values in the FCCS analysis showed that Sis1-prion interactions are stronger than Hsp104-prion interactions. This result is consistent with previous biochemical observation that the major components of cellular Sup35 aggregates were Sup35 and Sis1 (25). Consequently, our study demonstrats that the formation of the heterocomplex of prion oligomers may be a common event in prion cells, even though only a part of the known prion proteins was examined in this study.

MATERIALS AND METHODS

Detailed information is provided in the Supplementary Material.

ACKNOWLEDGMENTS

We thank Roger Tsien (UCSD) for the *mCherry* gene. This work was supported by National Institutes of Health Grant GM53655 and the USDA Cooperative State Research, Education and Extension Service (CSREES) project WISO4769 (to E.A.C.); Human Frontier Science Program Long-Term Fellowship (T.H.)

CONFLICTS OF INTEREST

Authors have no conflicting financial interests.

FIGURE LEGENDS

Figure 1. Unique and similar diffusional properties of prion oligomers in live cells. (*A*) Representative normalized fluorescence auto-correlation functions (FAFs) of mGFP (*black*), Sup35NM-GFP (*blue*), Sup35-GFP (*red*) in yeast lysates prepared from non-prion cells are shown (circle symbol). (*B*) Representative normalized FAFs of mGFP (*gray*) detected in [*psi* $^{-}$] cell, Sup35NM-GFP in [*psi*$^{-}$] (*black*) and [*PSI*$^{+}$] (*blue*) cells, and Sup35-GFP in [*gpsi*$^{-}$] (*green*) and [*GPSI*$^{+}$] (*red*) cells are respectively shown. For comparison of mobility, all of the curves were normalized to the same amplitude, G (0) = 2. Solid lines indicate fitting of two-component models to the results. (*C*) and (*D*) Plot of diffusion times versus the corresponding fractional ratios of Sup35NM-GFP and Sup35-GFP (Sup35NMGC) in [*PSI*$^{+}$] and [*GPSI*$^{+}$] prion cells are respectively shown. Two types of diffusion times (τ_i, i=2) were evaluated from two-component model fitting (*see also Methods*). Fast diffusion time (solid circle) and slow diffusion time (open circle) are inversely proportional to diffusional coefficients of D_{fast} and D_{slow}, respectively (Table 1).

Figure 2. Stable interaction among prion proteins in live cells. (*A*) Representative confocal image of [*gpsi*$^{-}$] cells co-expressing Sup35NM-TagRFP and Sup35NGMC and (*B*) image of [*GPSI*$^{+}$] cells co-expressing Sup35NM- TagRFP and Sup35NGMC are shown (upper). Scale bar, 5μm. Representative FCCS measurement carried on cells are respectively shown (central and bottom). (Central) Time trace of average fluorescence intensity (counts per second; cps in kHz) of the two proteins. (Bottom) Two corresponding fluorescence auto-correlation functions (FAFs) of TagRFP signal (*red*) and GFP signal (*blue*), and one fluorescence cross-correlation function (FCF) are shown. Fit curves (solid line) from two-component analysis are also shown. (*C*) Mean values of relative cross-correlation amplitudes (RCA), representing interactions between Sup35NGMC with other prion proteins of Sup35NM-TagRFP, Ure2- TagRFP, Rnq-TagRFP, and New1-TagRFP, Trx-TagRFP in [*gpsi*$^{-}$] and [*GPSI*$^{+}$] cells, are shown. Thioredoxin-fused TagRFP (Trx-TagRFP), a non-prion related protein, expressed in [*gpsi*$^{-}$] and [*GPSI*$^{+}$] was used as negative control. Error bars represent the s.d. *P<0.05 compared with that of Sup35NM-TagRFP in [*GPSI*$^{+}$] cells.

Figure 3. Quantification of interaction between Sup35 oligomers and remodeling factors, Sis1 and Hsp104 in live cells. (*A*) Confocal image of [*PSI*$^{+}$] cells co-expressing Sis1-mCherry and Sup35NM-GFP

and (*B*) image of [*GPSI*$^{+}$] cells co-expressing Hsp104-mCherry and Sup35NGMC are shown (upper). Scale bar, 5μm. Representative FCCS measurement carried on the cells are shown (central and bottom). (*C*) Mean values of relative cross-correlation amplitudes (RCA) between Sis1-mCherry and Sup35NM-GFP in [*psi*$^{-}$] and [*PSI*$^{+}$] cells and between Sis1-mCherry and Rnq1-GFP in [*rnq*$^{-}$] and [*RNQ*$^{+}$] cells are shown. (*D*) Mean RCA values between Hsp104-mCherry and Sup35-GFP in [*gpsi*$^{-}$] and [*GPSI*$^{+}$], and GdnHCl treated [*GPSI*$^{+}$] cells during 6hr and 48 hr are shown. Error bars represent the s.d. *P<0.05 compared with that in non-treated [*GPSI* $^{+}$] cells.

REFERENCES

1. Prusiner SB (1998) Prions. Proc Natl Acad Sci U S A 95, 13363-13383
2. Wickner RB (1994) [URE3] as an altered URE2 protein: evidence for a prion analog in Saccharomyces cerevisiae. Science 264, 566-569
3. Tuite MF and Cox BS (2003) Propagation of yeast prions. Nat Rev Mol Cell Biol 4, 878-890
4. Tuite MF and Serio TR (2010) The prion hypothesis: from biological anomaly to basic regulatory mechanism. Nat Rev Mol Cell Biol 11, 823-833
5. Wickner RB, Edskes HK, Shewmaker F et al. (2007) Yeast prions: evolution of the prion concept. Prion 1, 94-100
6. Inoue Y (2009) Life cycle of yeast prions: propagation mediated by amyloid fibrils. Protein Pept Lett 16, 271-276
7. Taguchi H and Kawai-Noma S (2010) Amyloid oligomers: diffuse oligomer-based transmission of yeast prions. FEBS J 277, 1359-1368
8. Liebman SW and Chernoff YO (2012) Prions in yeast. Genetics 191, 1041-1072
9. Sondheimer N and Lindquist S (2000) Rnq1: an epigenetic modifier of protein function in yeast. Mol Cell 5, 163-172
10. Derkatch IL, Bradley ME, Hong JY and Liebman SW (2001) Prions affect the appearance of other prions: the story of [PIN(+)]. Cell 106, 171-182
11. Osherovich LZ and Weissman JS (2001) Multiple Gln/Asn-rich prion domains confer susceptibility to induction of the yeast [PSI(+)] prion. Cell 106, 183-194
12. Du Z, Park KW, Yu H, Fan Q and Li L (2008) Newly identified prion linked to the chromatin-remodeling factor Swi1 in Saccharomyces cerevisiae. Nat Genet 40, 460-465
13. Alberti S, Halfmann R, King O, Kapila A and Lindquist S (2009) A systematic survey identifies prions and illuminates sequence features of prionogenic proteins. Cell 137, 146-158
14. Suzuki G, Shimazu N and Tanaka M (2012) A yeast prion, Mod5, promotes acquired drug resistance and cell survival under environmental stress. Science 336, 355-359
15. Bradley ME, Edskes HK, Hong JY, Wickner RB and Liebman SW (2002) Interactions among prions and prion "strains" in yeast. Proc Natl Acad Sci U S A 99 Suppl 4, 16392-16399
16. Bosl B, Grimminger V and Walter S (2006) The molecular chaperone Hsp104--a molecular machine for protein disaggregation. J Struct Biol 156, 139-148
17. Doyle SM and Wickner S (2009) Hsp104 and ClpB: protein disaggregating machines. Trends Biochem Sci 34, 40-48
18. Masison DC, Kirkland PA and Sharma D (2009) Influence of Hsp70s and their regulators on yeast prion propagation. Prion 3, 65-73
19. Aron R, Higurashi T, Sahi C and Craig EA (2007) J-protein co-chaperone Sis1 required for generation of [RNQ+] seeds necessary for prion propagation. EMBO J 26, 3794-3803
20. Higurashi T, Hines JK, Sahi C, Aron R and Craig EA (2008) Specificity of the J-protein Sis1 in the propagation of 3 yeast prions. Proc Natl Acad Sci U S A 105, 16596-16601
21. Shorter J and Lindquist S (2008) Hsp104, Hsp70 and Hsp40 interplay regulates formation, growth and elimination of Sup35 prions. EMBO J 27, 2712-2724
22. Romanova NV and Chernoff YO (2009) Hsp104 and prion propagation. Protein Pept Lett 16, 598-605
23. Winkler J, Tyedmers J, Bukau B and Mogk A (2012) Chaperone networks in protein disaggregation and prion propagation. J Struct Biol 179, 152-160
24. Allen KD, Wegrzyn RD, Chernova TA et al. (2005) Hsp70 chaperones as modulators of prion life cycle: novel effects of Ssa and Ssb on the Saccharomyces cerevisiae prion [PSI+]. Genetics 169, 1227-1242
25. Bagriantsev SN, Gracheva EO, Richmond JE and Liebman SW (2008) Variant-specific [PSI+] infection is transmitted by Sup35 polymers within [PSI+] aggregates with heterogeneous protein composition. Mol Biol Cell 19, 2433-2443
26. Salnikova AB, Kryndushkin DS, Smirnov VN, Kushnirov VV and Ter-Avanesyan MD (2005) Nonsense suppression in yeast cells overproducing Sup35 (eRF3) is caused by its non-heritable amyloids. J Biol Chem 280, 8808-8812

27. Derkatch IL, Uptain SM, Outeiro TF, Krishnan R, Lindquist SL and Liebman SW (2004) Effects of Q/N-rich, polyQ, and non-polyQ amyloids on the de novo formation of the [PSI+] prion in yeast and aggregation of Sup35 in vitro. Proc Natl Acad Sci U S A 101, 12934-12939
28. Kaganovich D, Kopito R and Frydman J (2008) Misfolded proteins partition between two distinct quality control compartments. Nature 454, 1088-1095
29. Winkler J, Tyedmers J, Bukau B and Mogk A (2012) Hsp70 targets Hsp100 chaperones to substrates for protein disaggregation and prion fragmentation. J Cell Biol 198, 387-404
30. Saibil HR, Seybert A, Habermann A et al. (2012) Heritable yeast prions have a highly organized three-dimensional architecture with interfiber structures. Proc Natl Acad Sci U S A 109, 14906-14911
31. Kawai-Noma S, Ayano S, Pack CG et al. (2006) Dynamics of yeast prion aggregates in single living cells. Genes Cells 11, 1085-1096
32. Kawai-Noma S, Pack CG, Kojidani T et al. (2010) In vivo evidence for the fibrillar structures of Sup35 prions in yeast cells. J Cell Biol 190, 223-231
33. Kawai-Noma S, Pack CG, Tsuji T, Kinjo M and Taguchi H (2009) Single mother-daughter pair analysis to clarify the diffusion properties of yeast prion Sup35 in guanidine-HCl-treated [PSI] cells. Genes Cells 14, 1045-1054
34. Greene LE, Park YN, Masison DC and Eisenberg E (2009) Application of GFP-labeling to study prions in yeast. Protein Pept Lett 16, 635-641
35. Pack CG, Yukii H, Toh-e A et al. (2014) Quantitative live-cell imaging reveals spatio-temporal dynamics and cytoplasmic assembly of the 26S proteasome. Nat Commun 5, 3396

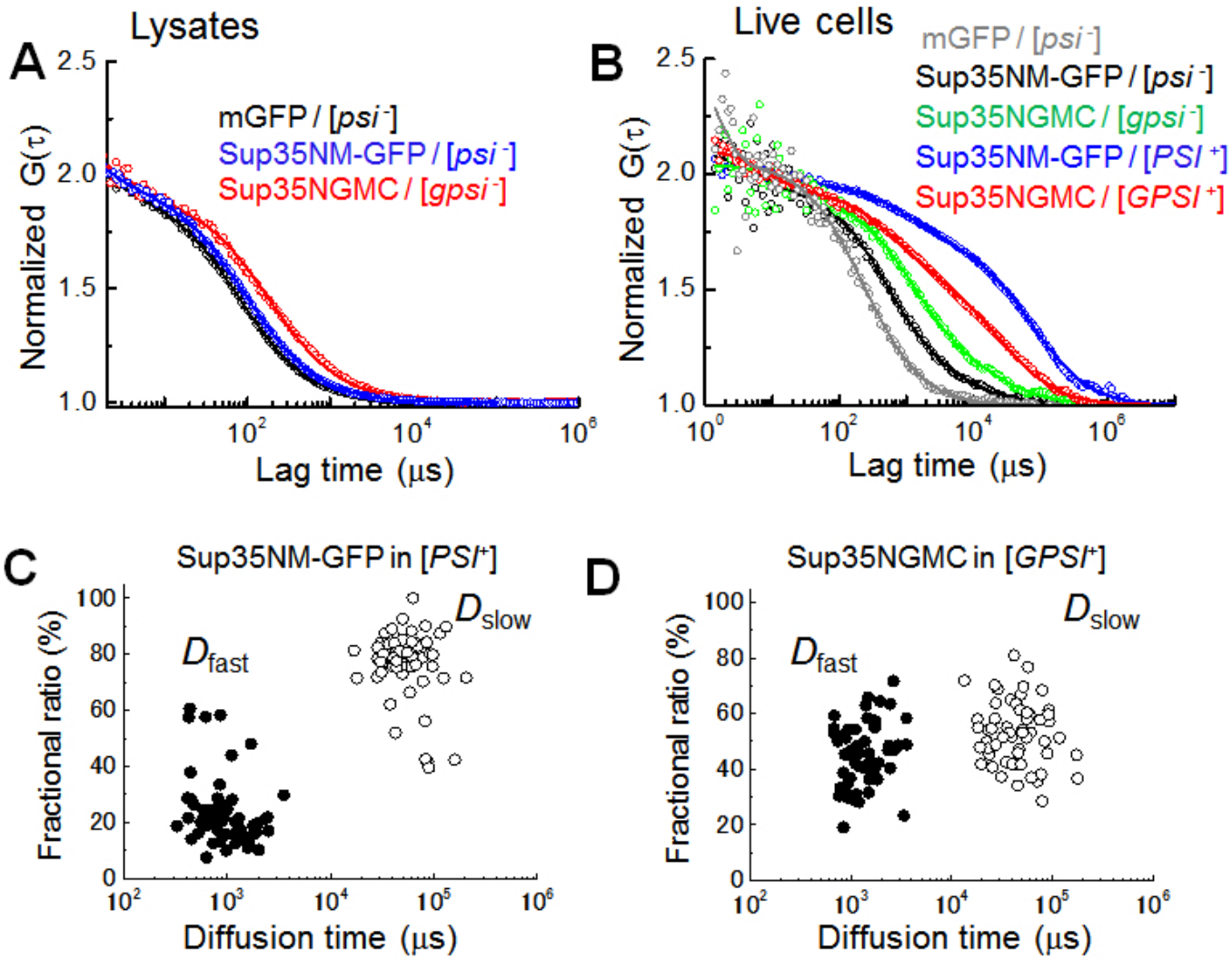

Fig. 1 Figure 1

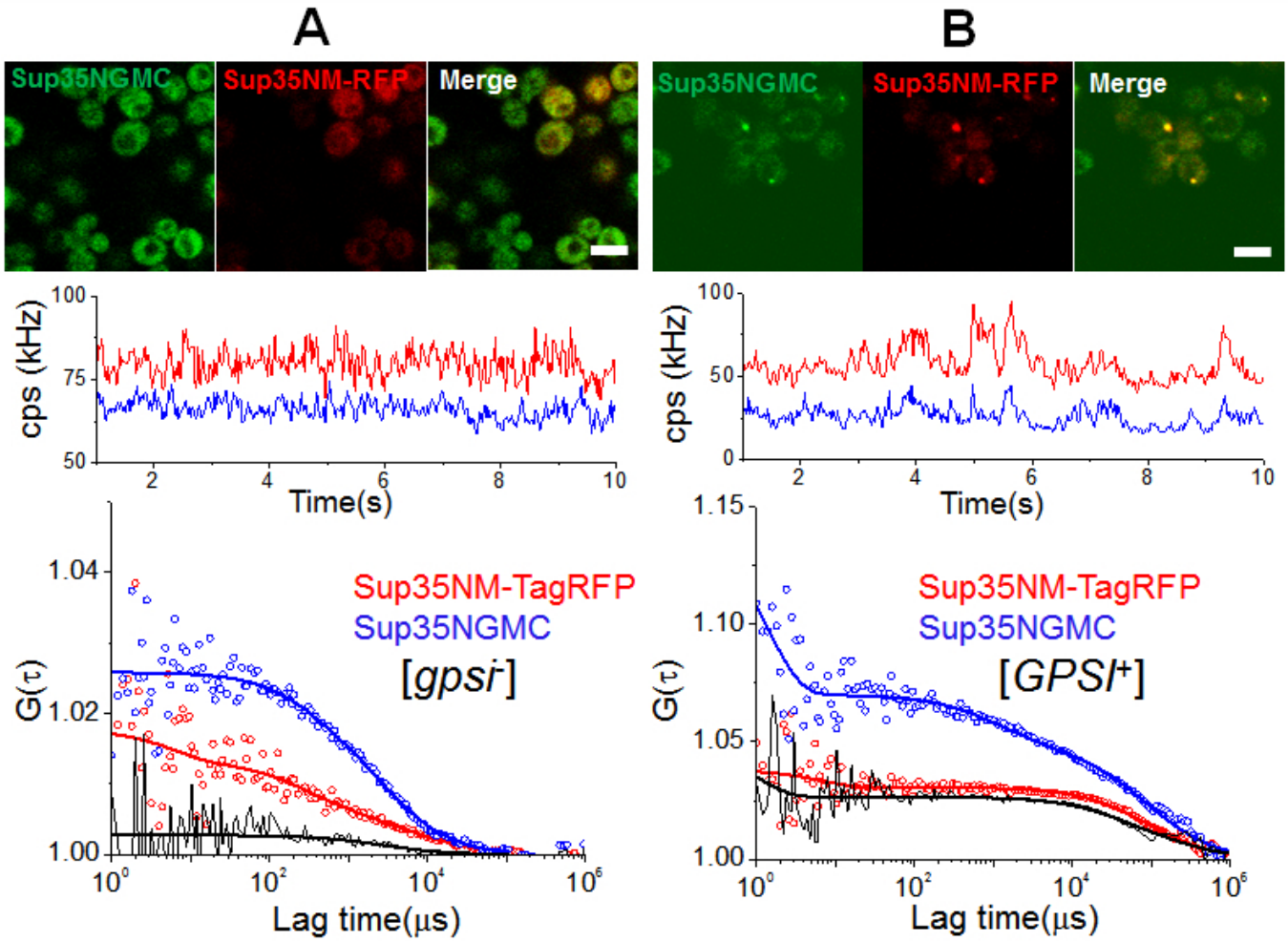

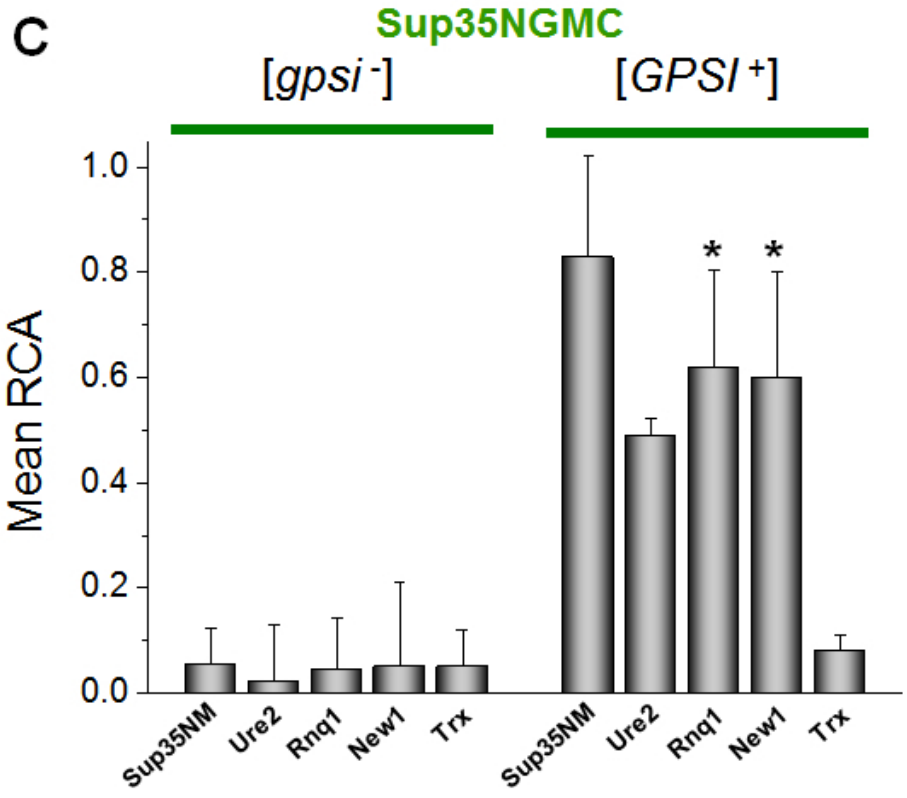

Fig. 2 Figure 2

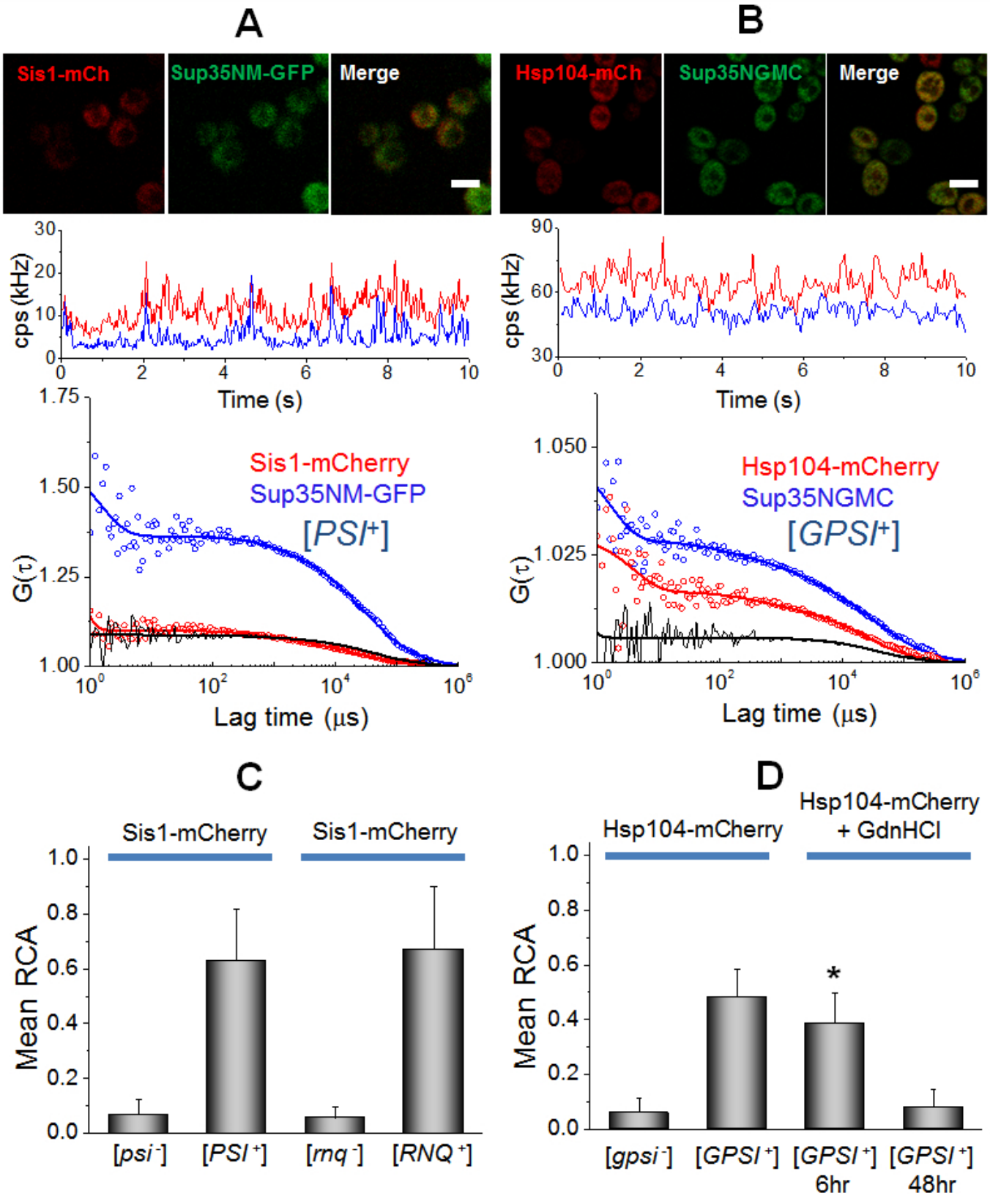

Fig. 3 Figure 3

TABLE

Table. Summary of *D* values for GFP, prion proteins and remodeling factors.

Type of sample	Probe molecule	D_{fast} ($\mu m^2 s^{-1}$)[a] (%)[b]	D_{slow} ($\mu m^2 s^{-1}$)[a] (%)[b]
[*psi*$^-$]	GFP (control)[c]	21.0 ± 3.8 (90)	0.26 ± 0.3 (10)
[*psi*$^-$]	Sup35NM-GFP	9.1 ± 1.5 (87)	0.26 ± 0.2 (13)
[*gpsi*$^-$]	NGMC	5.3 ± 2.1 (85)	0.18 ± 0.2 (15)
[*rnq*$^-$]	Rnq1-GFP	4.3 ±1.2 (90)	0.23 ± 0.2 (10)
[*PSI*$^+$]	GFP (control)[c]	18.2 ± 4.3 (89)	0.2 ± 0.3 (11)
[*PSI*$^+$]	Sup35NM-GFP	9.3 ± 2.8 (26)	0.12 ± 0.1 (74)
[*GPSI*$^+$]	NGMC	4.8 ± 1.9 (47)	0.15 ± 0.1 (53)
[*RNQ*$^+$]	Rnq1-GFP	4.8 ± 2.2 (23)	0.16 ± 0.1 (77)
Lysis solution	GFP ([*psi*$^-$], [*PSI*$^+$])[c]	77.0 ± 3.0 (100)	n.d.
	Sup35NM-GFP ([*psi*$^-$])	51.3 ± 3.7 (100)	n.d.
	Sup35NM-GFP ([*PSI*$^+$])	43.5 ± 12 (30)	3.3 ± 1.1 (70)
	NGMC ([*gpsi*$^-$])	31 ± 2.1 (100)	n.d.
	NGMC ([*GPSI*$^+$])	33 ± 3.1 (9)	6.2 ± 2.0 (91)
	Rnq1-GFP ([*rnq*$^-$])	56.3 ± 10.6 (100)	n.d
	Rnq1-GFP ([*RNQ*$^+$])	55.7 ± 6.4 (15)	2.9 ± 2.0 (85)
Non-prion cell	Hsp104-GFP	3.3 ± 1.6 (42)	0.34 ± 0.2 (58)
	Sis1-mCherry	11.0 ± 8.6 (65)	0.6 ± 0.3 (35)
Lysis solution	Hsp104-GFP	10.5 ± 1.0 (100)	n.d.
	Sis1-mCherry	18.0 ± 4.0 (100)	n.d.

[a] Diffusion coefficients were calculated from the FAF fitting result (means ± s.d.; cell number n=5).

[b] Fractional ratios corresponding to the diffusion coefficients are represented by percentage.

[c] Diffusion of GFP monomer in live yeast cells is shown as a reference.

Supplementary Materials

Heterogeneous interaction network of yeast prions and remodeling factors detected in live cells

Chan-Gi Pack[1,*], Yuji Inoue[2,#], Takashi Higurashi[3], Shigeko Kawai-Noma[2], Daigo Hayashi[2], Elizabeth Craig[3] & Hideki Taguchi[2]

[1] Asan Institute for Life Sciences, Asan Medical Center & Department of Convergence Medicine, University of Ulsan College of Medicine, Seoul 05505, Republic of Korea.

[2] Department of Biomolecular Engineering, Graduate School of Biosciences and Biotechnology, Tokyo Institute of Technology, B56, 4259 Nagatsuta, Midori-ku, Yokohama 226-8501, Japan.

[3] Department of Biochemistry, University of Wisconsin, 433 Babcock Drive Madison, WI 53706, USA.

[#] Present address: Department of Virology, Research Center for Infectious Diseases Control, Research Institute of Microbial Diseases, Osaka University, 3-1 Yamadaoka, Suita, Osaka, 565-0871, Japan

* Corresponding author

Chan-Gi Pack (Tel: 82-2-3010-8611, Fax: 82-3010-4182, E-Mail: changipack@amc.seoul.kr)

Running title: Interaction network of yeast prions in live cells

Abbreviations: Sup35NM, N and M domains of Sup35; Sup35NGMC, GFP tagged Sup35; Hsp, heat shock protein; CLSM, confocal laser scanning microscopy; FCS, fluorescence correlation spectroscopy; FCCS, fluorescence cross-correlation spectroscopy; RCA, relative cross-correlation amplitude

Supplementary Materials and Methods

Plasmid Construction

Open reading frame (ORF) sequences of *SUP35*, *RNQ1*, *URE2*, and *NEW1* genes were cloned directly from purified genomic DNA of *S. cerevisiae* BY4741 strain by a standard PCR method with appropriate pair of oligonucleotides. Each partial sequence corresponding to residues 1-253, 1-65 and 1-130 of Sup35, Ure2 and New1, respectively, was fused to the 5'-end of the sequence of *TagRFP* derived from pTagRFP-N (Evrogen) by an overlap-extension PCR method. Likewise, sequence corresponding to residues 134-405 of Rnq1 was fused to the 3'-end of the *TagRFP*-coding sequence. Finally, each chimeric DNA fragment was subcloned onto the pYES2 yeast expression plasmid vector (Invitrogen) to produce pYES-*SUP35NM-TagRFP*, pYES-*URE2N-TagRFP*, pYES-*NEW1N-TagRFP* and pYES-*TagRFP-RNQ1C*. As a negative control, a plasmid expressing thioredoxin-fused TagRFP (pYES-*Trx-TagRFP*) was also constructed by fusing the thioredoxin ORF originally coded on pThio-His B plasmid (Invitrogen) to the 5'-end of the TagRFP-coding sequence and subcloning onto pYES2 vector.

A plasmid that expresses Hsp104 fused with mCherry (pGAL1-*HSP104-mCherry*) was constructed as follows. The *HSP104* containing *Sac*I-*Bam*HI DNA fragment was cloned into YCplac111GAL1p (1). The *mCherry* DNA fragment was amplified from a pmCherry-N1 vector (Clontech) and inserted into the *Bam*HI-*Sal*I site of the YCplac111GAL1pHSP104 plasmid. This includes GS linker between *HSP104* and mCherry.

To visualize Sis1 in the yeast cell, pRS314-*SIS1p-SIS1-mCherry* was prepared. *SIS1* gene including *SIS1* own promoter was cloned from W303 PJ513a (2) and fused *mCherry* gene under *SIS1* gene with Gly-Ser linker by PCR. *SIS1p-SIS1-mCherry* construct was cloned to pRS314 (3) and used for plasmid shuffling to obtain Sis1-mCherry expression strains.

[*RNQ1p-RNQ1-GFP*] plasmid, pRS413-RNQ1p-RNQ1-GFP, was from our previous work (2).

A plasmid (pRS413CYC1p-SUP35NM-GFP) encoding Sup35NM-GFP under the control of CYC1 promoter was constructed with *SUP35NM* gene cloned from W303 PJ513a and monomeric GFP gene (2).

Yeast Strain

In this study, *S. cerevisiae* G74-D694 strain, which we have established previously (4) , was used as the parent strain. G74-D694 is a derivative of 74-D694 [*MAT***a**, *ade1-14(UGA), his3, leu2, trp1, ura3*] and carries a modified *SUP35* gene (*SUP35NGMC*), in which a GFP gene was integrated between the N and M domains of the endogenous *SUP35* gene. Either [*psi*$^-$] or [*PSI*$^+$] G74-D694, [*gpsi*$^-$] or [*GPSI*$^+$], respectively, was transformed with yeast expression plasmid described above by a standard lithium acetate method. Transformants were selected by synthetic medium lacking uracil (SC-Ura) or leucin (SC-Leu). To induce expression of each protein, 2% (w/v) galactose was added to synthetic medium containing 2% (w/v) raffinose instead of glucose and lacking uracil (SRaf (-ura)) for 4~ to 24h.

Details of W303 *sis1-Δ::LEU2* [*SIS1p-SIS1*] [*RNQ*$^+$] [*psi*$^-$] or [*rnq*$^-$] [*PSI*$^+$] strains were described previously (2, 5). BY4741 *MATa HSP104-GFP::HIS3MX6* was described in the previous study (6). W303 *sis1-Δ::LEU2* [*SIS1p-SIS1-mCherry*] strains with [*RNQ*$^+$] or [*PSI*$^+$] were prepared by plasmid shuffling. Growth and prion maintenance of W303 *sis1-Δ::LEU2* strain having expression of Sis1-mCherry was indistinguishable to W303 *sis1-Δ::LEU2* strain with that of wild-type Sis1 from a [*SIS1p-SIS1*] plasmid. To measure FCS/FCCS, prion-GFP plasmid, *pRS413-RNQ1p-RNQ1-GFP* for [*RNQ*$^+$]/[*rnq*$^-$] or *pRS413CYCp-SUP35NM-GFP* for [*PSI*$^+$]/[*psi*$^-$], was coexpressed in W303 *sis1-Δ::LEU2* [*SIS1p-SIS1-mCherry*]. Semi-denaturing detergent agarose gel (5, 7) pattern of the prion-GFP coexpression strains showed identical pattern as of strains without coexpression. W303 [*rnq*$^-$] and [*psi*$^-$] strains were

obtained by 3 mM guanidine HCl hydrochloride (GdnHCl) treatment in the appropriate media for 2 days.

Protein Expression

Transformed yeast cells were cultured in SRaf (-ura). At mid-log phase, protein expression was induced by the addition of galactose at a final concentration of 0.2%. After a 12-h incubation at 30°C, cells were used for FCCS measurement. To estimate the expression level of each fusion protein conveniently, we utilized the fluorescence of TagRFP. Fluorescence images at green and red channel of a 100-µl droplet of each culture fluid were taken by LAS-4000 luminescence imager (Fuji Film, Japan) and the relative TagRFP fluorescence was analyzed by Multi Gauge (Fuji Film, Japan).

Fluorescence Correlation Spectroscopy (FCS) and Fluorescence Cross-Correlation Spectroscopy (FCCS). FCS and FCCS measurements were performed at 25°C on a confocal microscope system (LSM 510; Carl Zeiss) combined with a ConfoCor2 (Carl Zeiss). For confocal imaging followed by FCS or FCCS measurement, GFP and RFP were scanned independently in a multi-tracking mode. Details of the combined microscope system, analysis of fluorescence auto- function (FAF) obtained from FCS measurement, and analysis of two FAFs and one cross-correlation function (FCF) from FCCS measurement were described in previous studies (1, 6). Briefly, FAF and FCF, from which the absolute number and diffusion coefficient (D) of mobile fluorescent molecules, fractional ratio, and interaction amplitude represented by relative cross-correlation amplitude (RCA) are calculated, are obtained as follows:

The fluorescence auto-correlation functions of the red and green channels, $G_r(\tau)$ and $G_g(\tau)$, and the fluorescence cross-correlation function, $G_c(\tau)$, were calculated from

$$G_x(\tau) = 1 + \frac{\langle \delta I_i(t) \cdot \delta I_j(t+\tau) \rangle}{\langle I_i(t) \rangle \langle I_j(t) \rangle} \quad (1)$$

where τ denotes the time delay, I_i is the fluorescence intensity of the red channel ($i = r$) or green channel ($i = g$), and $G_r(\tau)$, $G_g(\tau)$, and $G_c(\tau)$ denote the auto correlation function of red ($i = j = x = r$), green ($i = j = x = g$), and cross ($i = r, j = g, x = c$), respectively. The acquired $G_x(\tau)$s were fitted using a one-component model for solution samples and a two-component model for live cells:

$$G_x(\tau) = 1 + \frac{1}{N} \sum_i F_i \left(1 + \frac{\tau}{\tau_i}\right)^{-1} \left(1 + \frac{\tau}{s^2 \tau_i}\right)^{-1/2} \quad (2)$$

where F_i and τ_i are the fraction and diffusion time of component i, respectively. N is the average number of fluorescent particles in the excitation-detection volume defined by radius w_0 and length $2z_0$, and s is the structure parameter representing the ratio $s = z_0/w_0$. The structure parameter was calibrated using the known diffusion coefficient of Rhodamine-6G at room temperature ($280 \mu m^2 s^{-1}$). To estimate the diffusion coefficient and fractional ratio from FCS or FCCS measurements, FAF and FCFs in live cells were fitted by a two-component model (i=2, D_{fast} and D_{slow}) with a triplet term (6). Although the shape of FAFs originated from a one-component model (i.e. single-species) only depends on the diffusional mobility, it is emphasized that the shape of FAFs originated from a multi-component model (multi-species) depends not only on the diffusional mobility but also on fractional ratio of mobile species (1). For FCCS measurement, simultaneous excitation of GFP- and RFP-tagged proteins was carefully carried out at minimal and optimal excitation powers, chosen to obtain sufficiently high signal-to-noise ratios for the analysis of the diffusional coefficient and molecular interaction. Data containing severe photobleaching possibly resulting from a high proportion of immobilized fluorophores and non-stationary fluorescent signals resulting from

the drift of yeast cells were excluded from the analysis. For FCCS analysis, the amplitude of the cross-correlation function was normalized by the amplitude of the autocorrelation function of RFP to calculate the relative cross-correlation amplitude ((*Gc*(0)-1)/(*Gr*(0)-1); RCA value)(6).

Supplementary Table S1. Theoretical molecular weights of prion proteins, Sis1, and Hsp104.

Proteins	Theoretical Mw (kD)	FP tagged proteins	Total theoretical Mw (kD)	Mw_{fcs} [c]
		mGFP ,mCherry, TagRFP	28	25
Sup35NM	49	Sup35NM-GFP	77	79
Sup35	79	NGMC	107	350
Rnq1	43	Rnq-GFP	71	76
Ure2	40	Ure2-mCherry	68	-
New1	134	New1-Ure2-mCherry	162	-
Sis1	40	Sis1-mCherry	68 (136 [a])	1720
Hsp104	104	Hsp104-GFP	132 (792 [b])	8600

[a] Molecular weight of Sis1-GFP as a homo-dimer.

[b] Molecular weight of Hsp104-GFP as a hexamer complex.

[c] Mw calculated from FCS analysis using lysis solution samples.

Supplementary Table S2. Molecular concentrations of Sup35NM-GFP and Sup35NGMC proteins in yeast cells

Proteins and cell type	Concentration (nM)	SD (nM)
Sup35NM-GFP in [*psi*$^-$]	676	130
Sup35NGMC in [*gpsi*$^-$]	285	60
Sup35NM-GFP in [*PSI*$^+$]	193	20
Sup35 NGMC in [*GPSI*$^+$]	150	12

Supplementary Figure S1

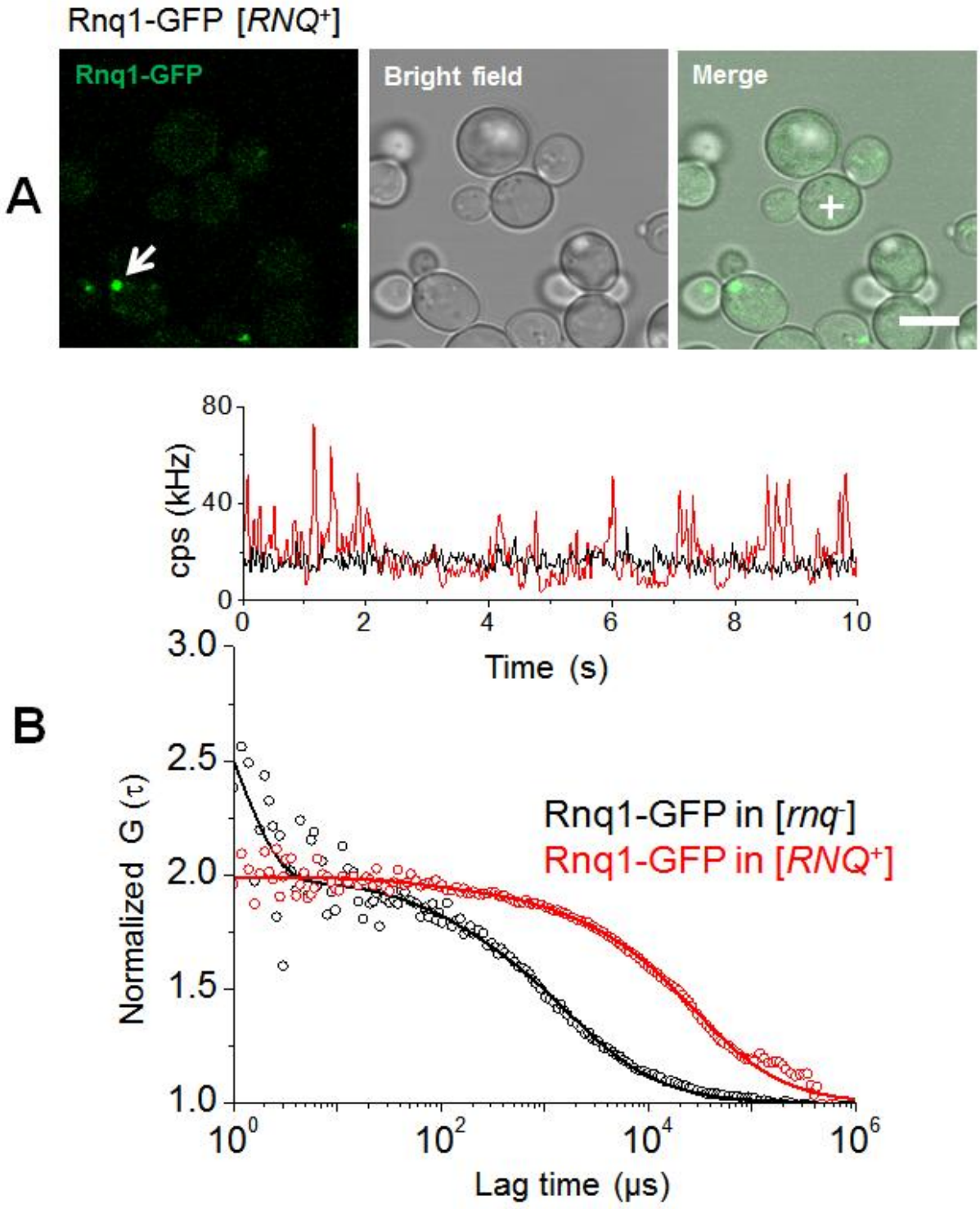

Supplementary Figure S2

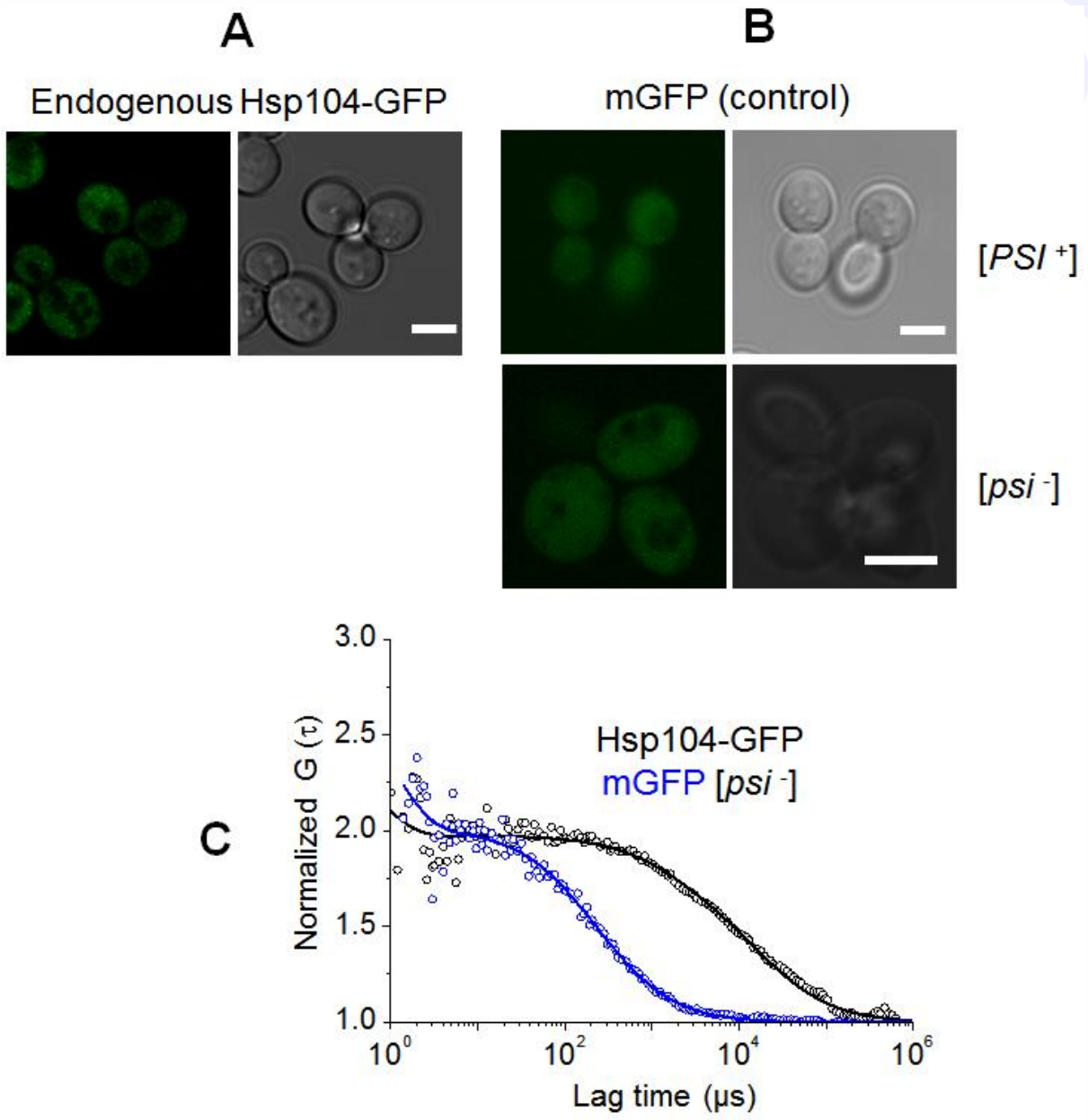

Supplementary Figure S3

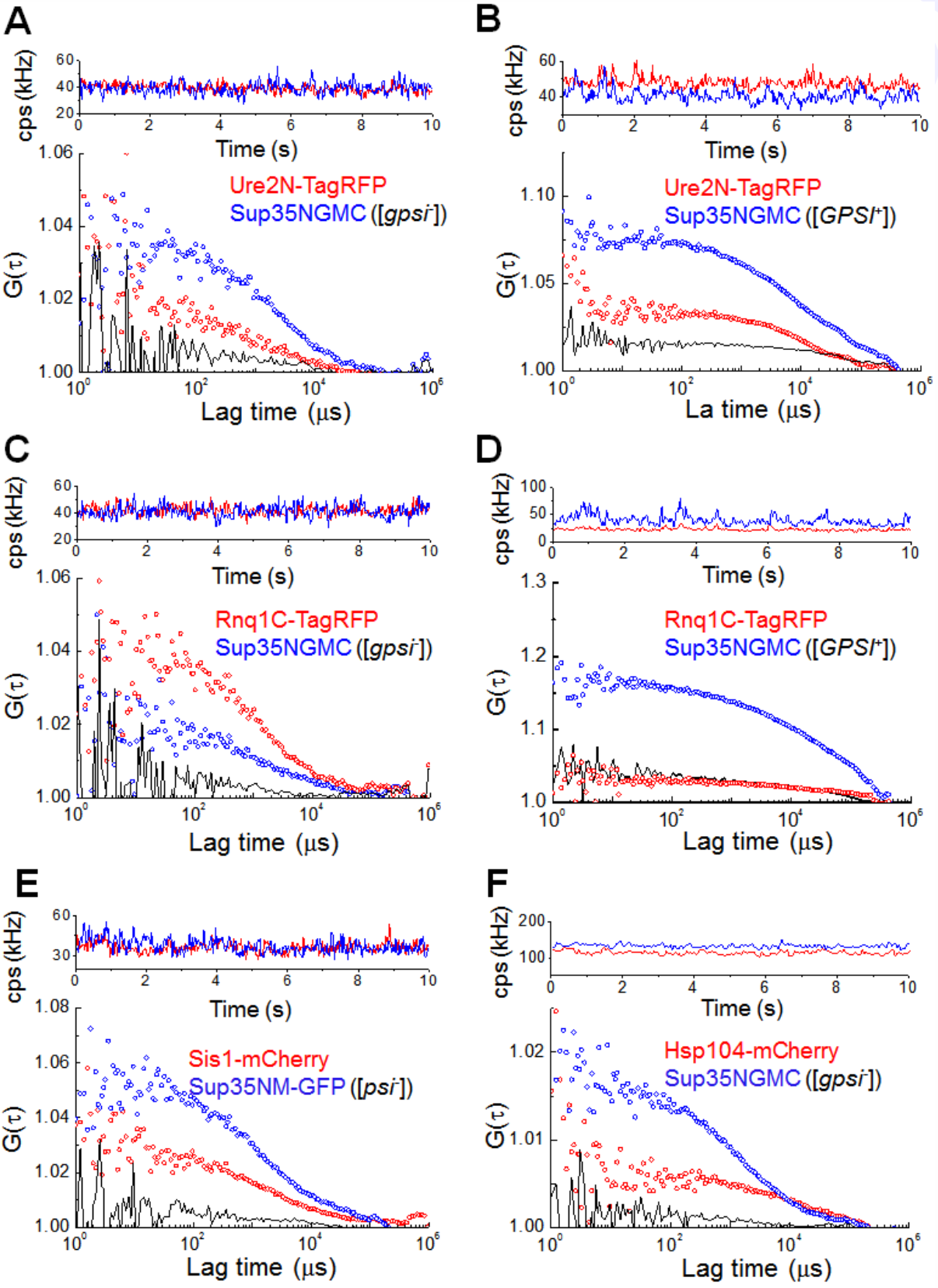

Supplementary Figure S4

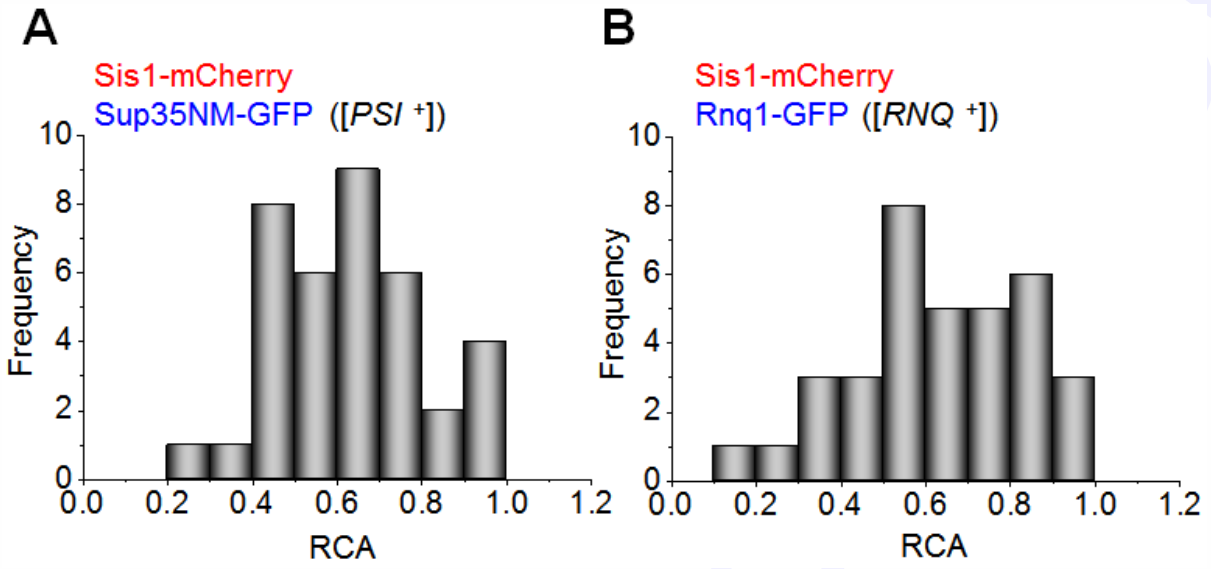

Supplementary Figure Legends

Supplementary Figure S1. Diffusional properties of Rnq1-GFP in live cells. (*A*) Fluorescence-confocal image of [*RNQ* $^{+}$] prion cells expressing Rnq1-GFP are shown. Scale bar, 5μm. Arrow and cross hair indicate a large immobile focus in a mother cell and the position of FCS measurement shown in (*B*), respectively. (*B*) Representative two FCS measurements carried on [*rnq* $^{-}$] and [*RNQ* $^{+}$] cells are respectively shown. (Upper) Time trace of average fluorescence intensity (counts per second; cps in kHz) of Rnq1-GFP observed in [*rnq* $^{-}$] (*black*) and [*RNQ* $^{+}$] (*red*) cells. (Bottom) The corresponding fluorescence auto-correlation functions (FAFs) calculated from the time trace are also shown. Fit curves (solid line) were obtained from two-component analysis. For comparison of mobility, the curves were normalized to the same amplitude, G (0) = 2.

Supplementary Figure S2. Slow diffusional behavior of Hsp104-GFP in non-prion cells. (*A*) Fluorescence-confocal image of yeast cells endogenously expressing Hsp104-GFP are shown. Scale bar, 5μm. (*B*) Fluorescence-confocal image of [*psi* $^{-}$] and [*PSI* $^{+}$] cells expressing monomer GFP (mGFP) are respectively shown. Scale bar, 5μm. (*C*) Representative normalized FAFs of Hsp104-GFP and mGFP are also shown. Fit curves (solid line) were obtained from two-component analysis. For comparison of mobility, the curves were normalized to the same amplitude, G (0) = 2.

Supplementary Figure S3. FCCS measurements for detecting interactions among prion proteins in live cells. (*A*) ~ (*D*) Representative FCCS measurement carried on non-prion and prion cells are respectively shown (upper and bottom). (Inset) Measured cell type ([*gpsi* $^{-}$] or [*GPSI* $^{+}$]) and a pair of proteins tagged with Tag-RFP and GFP. (Upper) Time trace of average fluorescence intensity (counts per second; cps in kHz) of two prion proteins (*red* and *blue*).

(Bottom) Two corresponding fluorescence auto-correlation functions (FAFs) of mCherry signal (*red*) and GFP signal (*blue*), and one fluorescence cross-correlation function (FCF) are shown. (E) Representative FCCS measurement carried on a [*psi* ⁻] cell co-expressing Sis1-mCherry and Sup35NM-GFP are shown. (F) Representative FCCS measurement carried on a [g*psi* ⁻] cell co-expressing Hsp104-mCherry and Sup35NGMC are shown.

Supplementary Figure S4. Histogram of RCA values for interaction between remodeling factor Sis1 and prion oligomers in yeast prion cells. (*A*) Histogram of RCA values for interaction between Sis1-mCherry and Sup35NM-GFP oligomers. (*B*) Histogram for interaction between Sis1-mCherry and Rnq1-GFP oligomers.

References

1. Kawai-Noma S, Ayano S, Pack CG et al. (2006) Dynamics of yeast prion aggregates in single living cells. Genes Cells 11, 1085-1096
2. Aron R, Higurashi T, Sahi C and Craig EA (2007) J-protein co-chaperone Sis1 required for generation of [RNQ+] seeds necessary for prion propagation. EMBO J 26, 3794-3803
3. Sikorski RS and Hieter P (1989) A system of shuttle vectors and yeast host strains designed for efficient manipulation of DNA in Saccharomyces cerevisiae. Genetics 122, 19-27
4. Tsuji T, Kawai-Noma S, Pack CG et al. (2011) Single-particle tracking of quantum dot-conjugated prion proteins inside yeast cells. Biochem Biophys Res Commun 405, 638-643
5. Higurashi T, Hines JK, Sahi C, Aron R and Craig EA (2008) Specificity of the J-protein Sis1 in the propagation of 3 yeast prions. Proc Natl Acad Sci U S A 105, 16596-16601
6. Pack CG, Yukii H, Toh-e A et al. (2014) Quantitative live-cell imaging reveals spatio-temporal dynamics and cytoplasmic assembly of the 26S proteasome. Nat Commun 5, 3396
7. Kryndushkin DS, Alexandrov IM, Ter-Avanesyan MD and Kushnirov VV (2003) Yeast [PSI+] prion aggregates are formed by small Sup35 polymers fragmented by Hsp104. J Biol Chem 278, 49636-49643